MOLECULAR AND CELLULAR BIOLOGY, Apr. 1994, p. 2391–2403
0270-7306/94/$04.00+0

Vol. 14, No. 4

NHP6A and *NHP6B*, Which Encode HMG1-Like Proteins, Are Candidates for Downstream Components of the Yeast *SLT2* Mitogen-Activated Protein Kinase Pathway

CHRISTINE COSTIGAN,[1] DAVID KOLODRUBETZ,[2] AND MICHAEL SNYDER[1]*

Department of Biology, Yale University, New Haven, Connecticut 06520-8103,[1] and Department of Microbiology, University of Texas Health Science Center, San Antonio, Texas 78284[2]

Received 5 October 1993/Returned for modification 22 November 1993/Accepted 19 January 1994

The yeast *SLK1* (*BCK1*) gene encodes a mitogen-activated protein kinase (MAPK) activator protein which functions upstream in a protein kinase cascade that converges on the MAPK Slt2p (Mpk1p). Dominant alleles of *SLK1* have been shown to bypass the conditional lethality of a protein kinase C mutation, *pkc1*-Δ, suggesting that Pkc1p may regulate Slk1p function. Slk1p has an important role in morphogenesis and growth control, and deletions of the *SLK1* gene are lethal in a *spa2*-Δ mutant background. To search for genes that interact with the *SLK1-SLT2* pathway, a synthetic lethal suppression screen was carried out. Genes which in multiple copies suppress the synthetic lethality of *slk1-1 spa2*-Δ were identified, and one, the *NHP6A* gene, has been extensively characterized. The *NHP6A* gene and the closely related *NHP6B* gene were shown previously to encode HMG1-like chromatin-associated proteins. We demonstrate here that these genes are functionally redundant and that multiple copies of either *NHP6A* or *NHP6B* suppress *slk1*-Δ and *slt2*-Δ. Strains from which both *NHP6* genes were deleted (*nhp6*-Δ mutants) share many phenotypes with *pkc1*-Δ, *slk1*-Δ, and *slt2*-Δ mutants. *nhp6*-Δ cells display a temperature-sensitive growth defect that is rescued by the addition of 1 M sorbitol to the medium, and they are sensitive to starvation. *nhp6*-Δ strains also exhibit a variety of morphological and cytoskeletal defects. At the restrictive temperature for growth, *nhp6*-Δ mutant cells contain elongated buds and enlarged necks. Many cells have patches of chitin staining on their cell surfaces, and chitin deposition is enhanced at the necks of budded cells. *nhp6*-Δ cells display a defect in actin polarity and often accumulate large actin chunks. Genetic and phenotypic analysis indicates that *NHP6A* and *NHP6B* function downstream of *SLT2*. Our results indicate that the Slt2p MAPK pathway in *Saccharomyces cerevisiae* may mediate its function in cell growth and morphogenesis, at least in part, through high-mobility group proteins.

Mitogen-activated protein kinase (MAPK) pathways function in the stimulation of growth and differentiation in response to extracellular signals (for reviews, see references 2 and 5). These pathways have been implicated in the transmission of signals propagated at the cell surface into changes in nuclear and cytoskeletal activities. Defining the targets of MAPK activity is therefore of fundamental importance for understanding at a molecular level how intracellular processes are dramatically altered in response to environmental signals.

MAPK pathways are composed of an array of protein kinases which act sequentially, ultimately stimulating the downstream MAPK to phosphorylate and activate a target protein(s) (2, 5). Stimulation of MAPK activity is mediated by phosphorylation at a conserved threonine and tyrosine located in the catalytic domain of the kinase (49). The phosphorylation of these two residues is carried out by a dual-specificity kinase, a MAPK kinase (MKK) (24, 51). In turn, MKK activity is regulated by phosphorylation. RAF and MAPK activators are two classes of kinases which regulate MKKs (14, 36, 37). The kinases which compose MAPK pathways in a variety of organisms and cell types have been identified (2, 5). This array of kinases has been aptly termed a signal transduction module, since the component kinases are often functionally conserved between species (47).

Recently, extensive effort has been devoted to identifying the downstream targets of activated MAPKs. Evidence has been presented that MAPKs can translocate between the nucleus and cytoplasm (10), and both nuclear and cytoplasmic substrates have been proposed for these enzymes. The transcription factors c-Jun (50), c-Myc (3, 57), and $p62^{TCF}$ (21) and ribosomal S6 kinase II (63), tyrosine hydroxylase (26), and cytosolic phospholipase A2 (43) can each serve as in vitro substrates for MAPKs, and their in vivo phosphorylation patterns correlate with activation of MAPK pathways. Additional in vivo evidence indicating that MAPKs are important for activation of c-Myc and cytosolic phospholipase A2 has been obtained by using DNA transfection experiments (43, 57). However, although progress in identifying possible substrates of activated MAPKs has been made, much remains to be learned about the downstream events caused by MAPK activation in vivo.

Saccharomyces cerevisiae is an attractive organism in which to identify and characterize MAPK targets, because it is readily manipulated by genetic techniques. Three different MAPK pathways have been identified in this yeast: the *KSS1/FUS3* pathway which functions in mating (13, 15, 19), the *HOG1* pathway which functions in growth on high-osmolarity media (8), and the *SLT2* (*MPK1*) pathway which we and others are studying (11, 12, 30, 38, 39, 41, 46, 48, 65). Components of the *SLT2* (*MPK1*) pathway appear to play a role in cell morphogenesis and growth control (11, 12, 46) and may contribute to cell wall integrity (40, 48, 65). The presumptive component kinases of the *SLT2* (*MPK1*) MAPK pathway have been identified by genetic suppression studies (30, 38, 39, 46). Two functionally redundant genes, *MKK1* and *MKK2*, encode

* Corresponding author. Mailing address: Department of Biology, Yale University, P.O. Box 208103, New Haven, CT 06520-8103. Phone: (203) 432-6139. Fax: (203) 432-6161. Electronic mail address: SNYMICP@yalevm.ycc.yale.edu.

TABLE 1. Yeast strains used in this study[a]

Strain	Genotype
Y753	*MAT***a** *ura3-52 lys2-801 ade2-101 trp1-901 leu2-Δ98 spa2-Δ1::TRP1 slk1-1* + p*SPA2/TRP1/SUP4/CEN*
Y431F$^-$	*MAT***a** *ura3-52 lys2-801 ade2-101 trp1-901 leu2-Δ98*
Y433	*MATα ura3-52 lys2-801 ade2-101 his3-Δ200 leu2-Δ98*
Y609	*MAT***a** *ura3-52 lys2-801 ade2-101 trp1-901 his3-Δ200 spa2-Δ2::TRP1*
Y760	*MAT***a** *ura3-52 lys2-801 ade2-101 trp1-901 his3-Δ200 slk1-Δ2::URA3*
Y762	*MAT***a** *ura3-52 lys2-801 ade2-101 trp1-901 his3-Δ200*
Y782	*MAT***a** *ura3-52 lys2-801 ade2-101 trp1-901 his3-Δ200 slk1-Δ1::TRP1*
Y783	*MAT***a** *ura3-52 lys2-801 ade2-101 his3-Δ200 leu2-Δ98 slt2-Δ10::LEU2*
Y831	*MAT***a** *ura3-52 lys2-801 ade2-101 trp1-901 leu2-Δ98 spa2-Δ1::TRP1 cdc10-10* + p*SPA2/TRP1/SUP4/CEN*
Y864	*MAT***a** *ura3 ade2 trp1-901 his3-Δ200 leu2-3,112 gal4-Δ gal80-Δ pLEXA-lacZ::URA3*
Y865/DKY453	*MATα ura3-52 trp1-289 his3-Δ1 leu2-3,112 gal2 gal10*
Y866/DKY533	*MATα ura3-52 trp1-289 his3-Δ1 leu2-3,112 gal2 gal10 nhp6A-Δ2::URA3*
Y867/DKY622	*MATα ura3-52 trp1-289 his3-Δ1 leu2-3,112 gal2 gal10 nhp6B-Δ1::HIS3*
Y868/DKY625	*MATα ura3-52 trp1-289 his3-Δ1 leu2-3,112 gal2 gal10 nhp6A-Δ2::URA3 nhp6B-Δ1::HIS3*
Y869/DKY608	*MATα ura3-52 trp1-289 his3-Δ1 leu2-3,112 gal2 gal10 nhp6A-Δ3::URA3 nhp6B-Δ3::HIS3*

[a] All strains, except Y864, are in the S288C genetic background.

MKKs (30), which are likely candidates to phosphorylate Slt2p (Mpk1p) (30, 38). *SLK1* (*BCK1*) (11, 12, 39) encodes a MAPK activator that may act on Mkk1p and Mkk2p (30). Finally, a dominant allele of *SLK1* (*BCK1*) was isolated as an extragenic suppressor of *pkc1*-Δ, suggesting that Pkc1p is an upstream regulator in the Slk1p-Mkkp-Slt2p pathway (39).

The target proteins of the Slt2p MAPK pathway have not been found. Identification of such targets would contribute to an understanding of how this MAPK directs downstream events, and how they, in turn, influence yeast cell growth. To attempt to identify downstream components of the Slt2p MAPK pathway, a screen for multicopy suppressors of *slk1* defects was carried out, and the *NHP6A* gene was isolated. Nhp6Ap was identified previously as a yeast nuclear protein with the extraction characteristics of a mammalian high-mobility-group (HMG) protein (35). The gene encoding this protein and a highly homologous second gene, *NHP6B*, were subsequently cloned (34). Both genes encode proteins with DNA-binding domains similar to those of HMG1 proteins, and both genes are transcribed (34). Here, we present the first phenotypic analysis of *nhp6*-Δ mutants. Cells from which Nhp6p function is deleted exhibit many phenotypes similar to those of *SLT2* pathway mutants, and genetic evidence suggests that *NHP6A* and *NHP6B* operate downstream of *SLT2*. *nhp6*-Δ mutants also exhibit novel defects in morphology and the cytoskeleton.

MATERIALS AND METHODS

Strains, media, and general methods. The yeast strains used in this study are listed in Table 1. Growth media and genetic manipulation of yeast strains were as described by Sherman et al. (58). Cloning protocols were as described by Sambrook et al. (55). A 10-μg amount of adenine per ml was used in yeast media limited for adenine (IADE). Plates containing 5-fluoroorotic acid (5-FOA) were made with standard yeast medium and were supplemented with 1 mg of 5-FOA per ml (6).

Isolation of high-copy-number suppressors of *slk1*-Δ. A yeast genomic DNA library (9) carried in the 2μm plasmid, YEp24, was transformed into the *slk1-1 spa2*-Δ + p*SPA2/SUP4/CEN* mutant (Y753) (11), and transformants were selected on IADE medium lacking uracil (11) at 24°C. Of 57,000 transformants, 73 sectoring colonies were identified by visual screening of plates under ×10 magnification. Sectoring transformants were plated on IADE plates lacking uracil, and red colonies were isolated. To ensure that the ability to lose the p*SPA2/SUP4/CEN* plasmid was due to the presence of the genomic clone in YEp24 and not a chromosomal mutation, the red colonies were then streaked on 5-FOA plates. Of the 73 red colonies derived from different transformants, 21 grew on the 5-FOA plates, indicating that they did not require the suppressor plasmid for growth; these strains were discarded. Plasmids from the remaining red colonies were rescued into *Escherichia coli* and retested for suppressor activity by transformation into Y753; all plasmids restored sectoring.

The 52 suppressor plasmids were analyzed by restriction mapping, and the genomic DNA inserts fell into five classes. The largest class of suppressor plasmids had 43 members (including eight different clones) and contained the *SLK1* gene. Plasmid DNAs from the remaining four classes of suppressors were transformed into the *slk1*-Δ strain, Y782, and into the *spa2*-Δ *cdc10-10* + p*SPA2/SUP4/CEN* strain, Y831 (18). One suppressor conferred red sectoring in *spa2*-Δ *cdc10-10* + p*SPA2/SUP4/CEN* and was classified as a *spa2*-Δ suppressor. The remaining three suppressors could suppress *slk1*-Δ; these suppressor DNAs were transformed into the *slt2*-Δ strain, Y783.

To identify the region of each plasmid that encoded the suppressor activity, individual restriction fragments were subcloned into the multicopy (2μm) vector YEp352 (28) and were then tested for the ability to confer red sectoring in Y753. Erase-a-Base reactions (Promega Biotec) (27) were performed on fragments in YEp352 to generate deletion constructs for further mapping and for sequence analysis. Sequencing reactions (56) were performed with the Universal Primer and Reverse Primer (U.S. Biochemicals). Approximately 500 nucleotides of sequence from the suppressing regions were compared with sequences in the GenBank DNA data base. The *spa2*-Δ suppressor and two of the *slk1*-Δ suppressors are novel yeast genes whose characterization will be reported elsewhere. The remaining *slk1*-Δ suppressor mapped to a 588-bp *Kpn*I-*Nde*I fragment which contains the previously described *NHP6A* gene (34). Deletion of the 99-bp *Kpn*I-*Bst*EII fragment, which removes the 5′ flanking DNA and the first three codons of the *NHP6A* coding sequence, abolished the ability of this suppressor to rescue the *slk1*-Δ mutant defects.

Deletion alleles of *SLT2*, *NHP6A*, and *NHP6B*. The *nhp6A*-Δ*2*, *nhp6A*-Δ*3*, *nhp6B*-Δ*1*, and *nhp6B*-Δ*3* alleles were constructed by standard cloning techniques and were transformed into yeast cells to replace the chromosomal copies (52). In *nhp6A*-Δ2, the 492-bp *Bst*EII-*Nae*I fragment which contains

the entire coding sequence for the *NHP6A* ORF (open reading frame) was replaced with the *URA3* gene; this deletion also removes parts of the C terminus and promoter, respectively, of the adjacent genes, *MAK3* and *ORF2* (64). An internal deletion of the *NHP6A* gene, *nhp6A-Δ3*, was generated by replacing the 129-bp *Bst*EII-*Eco*RV fragment which contains sequence encoding the N-terminal 45 amino acids of the ORF with the *URA3* gene. The *nhp6B-Δ1* allele replaced the *Sca*I-*Stu*I fragment of *NHP6B* with the *HIS3* gene. This deletion removes 66 codons of the ORF and 45 bp of 5′ flanking sequences. The *nhp6B-Δ3* mutation is an insertion of the *HIS3* gene at the *Bam*HI site of *NHP6B* and interrupts the gene after codon 23.

The *nhp6A-Δ* and *nhp6B-Δ* mutations were individually transformed into a wild-type diploid strain. Haploid *nhp6A-Δ* and *nhp6B-Δ* segregants that were recovered were indistinguishable from the wild type. A doubly heterozygous strain, *NHP6A/nhp6A-Δ NHP6B/nhp6B-Δ*, was also created. The *nhp6A-Δ nhp6B-Δ* segregants grew at 30°C, failed to grow at 38°C, grew at 38°C in the presence of 1 M sorbitol, were sensitive to nitrogen starvation, and formed aberrant morphologies at the restrictive temperature, i.e., they exhibited the same phenotypes as the double mutants generated by disruption in a haploid. Double mutant strains used in this study were generated by gene disruption in the haploid strain, Y865 (7). Correct substitutions at the chromosomal loci of *NHP6A* and *NHP6B* were confirmed by DNA gel blot analysis. In addition, a plasmid containing only the *NHP6A* gene complements the *nhp6A-Δ3 nhp6B-Δ3* double mutant, indicating that defects in the *nhp6A-Δ3 nhp6B-Δ3* mutant are attributable to *nhp6-Δ* and not some spurious mutation. Except for the analysis of morphological and cytoskeletal defects, all phenotypic analyses of *nhp6A-Δ nhp6B-Δ* double mutants were carried out on both the *nhp6A-Δ2 nhp6B-Δ1* and the *nhp6A-Δ3 nhp6B-Δ3* strains, and in all cases no differences between these strains were observed. The analysis of morphological and cytoskeletal defects was performed only on the *nhp6A-Δ3 nhp6B-Δ3* strain.

The *slt2-Δ10::LEU2* disruption mutation was created by cloning the *Bgl*II-*Hin*dIII fragment which contains the 5′ coding sequence of *SLT2* into the *Bam*HI-*Hin*dIII sites of the YIp vector, pRS305 (59). A *Sac*I-*Xba*I fragment which contains the 3′ coding sequence of *SLT2* was then cloned into the same vector at the *Sac*I-*Xba*I sites. This construct substitutes the 376 bp of the middle of the *SLT2* coding sequence with the *LEU2* plasmid DNA. The *slt2-Δ10* mutation construct was linearized with *Xba*I and transformed into the diploid yeast strain Y431F$^-$ × Y433. Haploid *slt2-Δ* segregants of a diploid transformant were generated by standard sporulation and dissection protocols (58). Correct substitution at the chromosomal locus of *SLT2* was confirmed by DNA gel blot analysis.

Synthetic lethality of *slt2-Δ spa2-Δ*. Possible synthetic lethality of *slt2-Δ spa2-Δ* was tested by dissecting 19 tetrads of a *MAT***a**/α *spa2-Δ/SPA2 slt2-Δ/SLT2* diploid. After growth at 24°C, segregants showed the following segregation pattern of live to dead progeny: 1 tetrad yielded 4 viable:0 dead progeny, 10 tetrads segregated 3:1, and 8 tetrads segregated 2:2. Of the viable spores, 13 were *slt2-Δ*, 17 were *spa2-Δ* and 0 were *slt2-Δ spa2-Δ* mutants, thus establishing that the *slt2-Δ spa2-Δ* double mutant is nonviable.

Multicopy vectors containing *NHP6B*, *PKC1*, *SLK1*, and *SLT2*. A 1.8-kb fragment containing the full-length *NHP6B* coding sequence and ~600 bp of 5′ and ~700 bp of 3′ flanking DNA was cloned into YEp352 (28). The *PKC1* gene carried in YCp50 was rescued from DL106 (41) into *E. coli*. An ~4.2-kb *Sph*I *PKC1* fragment was subcloned into YEp351, a 2μm *LEU2* vector (28). *SLK1* carried in a 2μm *LEU2* vector was isolated in a screen for multicopy suppressors of *slk1-Δ* (genomic DNA library in 2μm *LEU2* was provided by S. Roeder [16]) and contains the full-length *SLK1* gene and flanking DNA (4). An ~2.2-kb *Sal*I-*Kpn*I *SLT2* fragment was subcloned from YCp50:*SLT2* (46) into YEp351.

Microscopic analyses. Cell cultures were grown to early log phase (~3 × 10^6 cells per ml) in yeast extract-peptone-dextrose (YPD) at 30°C, which was then shifted to 38°C, and the cultures were incubated with shaking in a water bath. Aliquots were taken at regular intervals for analysis of cell density (optical density at 600 nm) and for fixation and microscopic analysis. Cells were fixed directly in growth media by the addition of formaldehyde to 3.7% and then pelleted and rinsed with phosphate-buffered saline (PBS) (0.15 M NaCl, 50 mM $NaPO_4$ [pH 7.4]) several times. Calcofluor and rhodamine-phalloidin staining was carried out similarly to the method described by Madden et al. (45). Cells were stained with Calcofluor by resuspension in 0.5 μg of Fluorescent Brightener no. 28 (Sigma) per ml. F actin was stained by resuspending cells in PBS, adding an equal volume of 3.3 mM rhodamine-phalloidin in methanol (Molecular Probes), incubating for ~3 h in the dark, briefly rinsing in PBS, and resuspending cells in 70% glycerol–PBS–2% *n*-propyl gallate. Criteria for quantitation of morphological defects are as follows: (i) enlarged necks refers to cells with ≥2× the wild-type neck diameter, and (ii) elongated buds refers to cells with ≥2× the maximum wild-type bud length. Criteria for quantitation of aberrant chitin are enhanced Calcofluor staining at the neck at cytokinesis and/or one or more aberrant, sharply defined Calcofluor-stained patches. The term actin chunks refers to large spots which stain with rhodamine-phalloidin and are ≥3× the size of wild-type actin spots. Changes in morphology and the distribution of chitin and actin were quantitated for cell aliquots obtained throughout incubation at the restrictive temperature, and the results were confirmed by three separate experiments. Values between separate experiments differed by less than 5%. Although cells were monitored over extended time periods, for clarity of presentation only values from several time points are cited to illustrate trends observed in the cell populations over time. Cells were also stained with methylene blue, which stains dead cells, to ensure that cell viability did not significantly decrease over the course of these experiments (>95% viable cells).

Shmoo formation was assayed as described elsewhere (11). The efficiency of shmoo formation was determined by counting at least 300 cells in a population that had been maintained at 30°C for 2.5 h in 8 μg of α-factor (Sigma) per ml. Assay of *nhp6* shmoo formation was performed by using a *MAT***a** *nhp6A-Δ nhp6B-Δ* segregant obtained from sporulation and dissection of a Y869 × Y609 diploid.

Scanning electron microscopy was performed by a variation of the procedure described by Gimeno et al. (22). Cells grown to an optical density at 600 nm of 0.3 were prepared by centrifugation from the culture medium, rinsed once in PBS, resuspended in 2.5% glutaraldehyde–0.1 M sodium cacodylate (pH 7.2), and incubated at 24°C for 1 h. Fixed cells were then rinsed once in 0.1 M sodium cacodylate (pH 7.2), resuspended in 1/30 the original culture volume with 0.1 M sodium cacodylate (pH 7.2), and drops were put on (1 mg/ml) polylysine-coated coverslips. Cells were allowed to settle on the coverslips for 0.5 h at 24°C. The coverslips were dehydrated in an ethanol series (50, 70, 80, 95, and 100% for four times), critical-point dried, mounted, and gold-palladium sputter coated. Cells were observed under ×6,000 to ×16,000 magnification in an ISI SS-40 scanning electron microscope.

Analysis of interactions in vivo by the yeast two-hybrid screen. The full-length coding sequence of the *SLT2* gene with

*Bam*HI sites introduced for cloning purposes was generated by PCR (53, 54) with primers 1 (5′-CGCGGATCCAGATGGCT GATAAGATAGAGAGGCAT-3′) and 2 (5′-CCAGGATC CCCGGTTACTTATAGTTTTTTGTCC-3′). Similarly, the full-length coding sequence of the *NHP6A* gene with *Bam*HI sites was cloned by PCR with primers 3 (5′-CGGGATCCCAA TGGTCACCCCAAGAGAACCTAAGAA-3′) and 4 (5′-CA GGATCCAAAAACGCGGGGAGGAAGTATCCCTA A-3′). The *SLT2* and *NHP6A* PCR fragments were digested with *Bam*HI and cloned into the *Bam*HI site of the pSH2-1 vector which contains the DNA fragment encoding the DNA-binding domain of LexA (codons 1 to 87) under the control of the *ADH1* promoter (23). The *SLT2* gene was also cloned into the *Bam*HI site of the pGAD2F vector which contains the DNA fragment encoding the transcriptional activation domain of Gal4p (codons 768 to 881) under the control of the *ADH1* promoter (17a). The junctions of the resulting fusions were checked by DNA sequencing. The p*GAL4*::*SLT2* construct was able to restore growth at 37°C to an *slt2* strain (*slt2-1 leu2* [received from C. Mann]), and the p*LexA*::*NHP6A* and p*LexA*::*SLT2* constructs were able to restore growth at 37°C to the slt2-Δ strain, Y783. Test plasmids and appropriate control plasmids were transformed into a strain containing the *lexA*::*lacZ* reporter gene (Y864).

Assay for β-galactosidase activity. Transformants were patched onto media selective for the plasmids, incubated at 24°C to allow growth of the patches, and then replica plated to a sterile Whatman 1-mm-pore-size filter on fresh selective media, and the strains were incubated again to allow growth of the patches on the filter. The patches were permeabilized by incubating the filter in a chloroform chamber for 10 min. The filter was then placed on an X-Gal (5-bromo-4-chloro-3-indolyl-β-D-galactopyranoside) indicator plate (100 mM sodium phosphate [pH 7], 1 mM $MgSO_4$, 120 μg of X-Gal per ml, 2% agar), incubated overnight at 24°C, and monitored for the development of blue color. Quantitative assays were then performed on strains grown in liquid culture (69). Strains to be assayed were always compared with appropriate positive (Y864 transformed with pSH17-4, which encodes a LexA::Gal4p fusion in pSH2-1 [24a] with or without pGAD2F) and negative (Y864 transformed with pGAD2F and/or pSH2-1) control strains. Qualitative assays were performed on at least three independent transformants of each strain; quantitative assays were performed on two different transformants of each strain. Similar results were obtained by both qualitative and quantitative assays.

Construction and analysis of the HA epitope-tagged form of Nhp6Ap. The *NHP6A* gene with DNA encoding an in-frame hemagglutinin (HA) epitope introduced at the 5′ end was generated by PCR with primer 5 (5′-CACCGGTAACCTAC CCTTATGATGTCCCAGATTACGCCGTCACCCCAAGA GAACCTAAGAAGAGA-3′) and primer 4 described above. Primer 5 encodes the nine-amino-acid HA epitope YPYDVP DYA (68), which is recognized by the mouse monoclonal antibody 12CA5 (BABCO). YEp352 containing the full-length *NHP6A* gene was digested with *Bst*EII and *Bam*HI to remove the *NHP6A* ORF (the *Bam*HI site lies in the YEp352 polylinker and is 3′ to the *NHP6A* gene). The resulting fragment which contained YEp352 and the promoter and ATG of *NHP6A* was ligated to the *HA*::*NHP6A* PCR fragment which had been digested with *Bst*EII and *Bam*HI. The fusion was checked by DNA sequencing, and expression of the HA::Nhp6Ap fusion protein was checked by immunoblot analysis as described by Snyder (61) and by immunoprecipitation as described in Harlow and Lane (25) using antibody 12CA5. Complementation assays with HA::Nhp6Ap were carried out by transforming *slk1*-Δ (Y782), *slt2*-Δ (Y783), and *nhp6A*-Δ *nhp6B*-Δ (a *ura3* revertant of Y869).

Metabolic labelling experiments were performed with three different strains: (i) a wild-type strain ($Y431F^-$) carrying *NHP6A* in YEp352, (ii) a wild-type strain ($Y431F^-$) carrying *HA*::*NHP6A* in YEp352, and (iii) a *slt2*-Δ strain (Y783) carrying *HA*::*NHP6A* in YEp352. Cells were grown overnight at 30°C to early exponential phase in 50 ml of medium lacking uracil and phosphate depleted as described by Warner (67). Cells were then pelleted, resuspended in 50 ml of phosphate-depleted YPD, and incubated for 2 h. Cells were again pelleted, resuspended in 6 ml of fresh phosphate-depleted YPD, and split into two tubes. To one tube, $H_3{}^{32}PO_4$ (ICN) was added to 0.2 mCi/ml. The other tube served as a nonradioactive positive control for immunoprecipitation of HA::Nhp6Ap and was treated identically to the first tube. Cells were incubated at 33°C for 0.5 h and then pelleted, rinsed twice in a solution containing PBS, 1 mM phenylmethylsulfonyl fluoride, 20 mM NaF, and 1 mM orthovanadate, and frozen in a dry ice-ethanol bath. Cell lysates and immunoprecipitations were carried out in the presence of protease inhibitors (1 mM phenylmethylsulfonyl fluoride and 2 μg each of chymostatin, leupeptin, and pepstatin per ml), RNase A (0.7 μg/μl), and phosphatase inhibitors (20 mM NaF, 1 mM orthovanadate). The ^{32}P-labelled samples were analyzed by autoradiography after sodium dodecyl sulfate-polyacrylamide gel electrophoresis (SDS-PAGE); the nonradioactive samples were analyzed by SDS-PAGE and immunoblot analysis with antibody 12CA5.

RNA (Northern) blot analysis. RNAs were prepared from exponentially growing wild-type (Y762), *slk1*-Δ (Y760), *slt2*-Δ (Y783), and *nhp6A*-Δ *nhp6B*-Δ (Y869) cells, separated in an agarose gel containing formaldehyde, and blotted as described elsewhere (32, 55). RNA samples were split into three aliquots and probed for *NHP6A*, *NHP6B*, and *ACT1*. Hybridization was detected with the Genius system (Boehringer). As expected, no hybridization of the *NHP6* probes was seen with the *nhp6A*-Δ *nhp6B*-Δ RNA sample. RNA was quantitated by densitometric analysis. *NHP6A* RNA levels were normalized by determining the ratio of *NHP6A* RNA to *ACT1* RNA.

RESULTS

Identification of multicopy suppressors of *slk1-1 spa2*-Δ synthetic lethality. The *SLK1* and *SPA2* genes both have a role in yeast morphogenesis (11, 20, 61). Slk1p is a kinase which is involved in cell morphogenesis and the control of cell growth (11, 12). Spa2p is a protein which colocalizes with sites of polarized cell growth (20, 61, 62). Neither gene is essential, but deletion of both genes results in cell death (synthetic lethality) (11). The Slk1p and Spa2p proteins are thought to operate in different pathways within the budding process; multiple copies of *SPA2* fail to suppress the *slk1*-Δ defects, and, conversely, multiple copies of *SLK1* fail to suppress *spa2*-Δ defects (data not shown).

We carried out a screen to isolate genes which, when present in multiple copies, suppress the lethality of *slk1-1 spa2*-Δ (i.e., a synthetic lethal suppression screen). It seemed probable that genes identified by this screen might encode proteins acting downstream of Spa2p, downstream of Slk1p, downstream of both Slk1p and Spa2p, or in a pathway redundant to those in which Slk1p and Spa2p function.

Previously, we had constructed a strain which has the following relevant markers: *spa2*-Δ*1*, *slk1-1*, *ade2-101*, and a p*SPA2/SUP4/CEN* plasmid (11). *spa2*-Δ*1* is a chromosomal deletion of the *SPA2* gene, *slk1-1* is a nonsense mutation in *SLK1* (*BCK1*), and *ade2-101* is a mutation in the *ADE2* gene

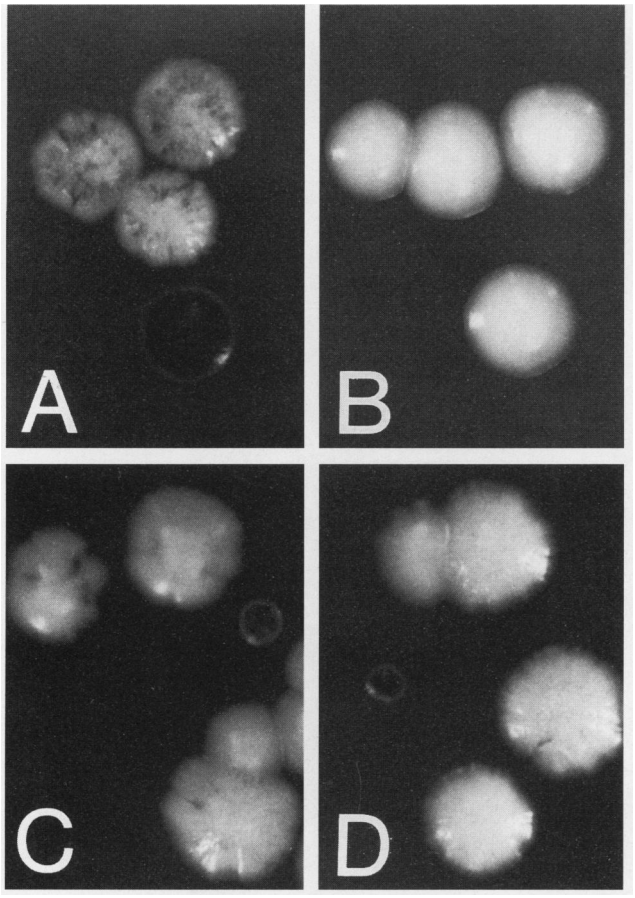

FIG. 1. Multiple copies of the *NHP6A* and *NHP6B* genes partially rescue *slk1-1 spa2*-Δ lethality; an *slk1-1 spa2*-Δ + p*SPA2/SUP4/CEN* strain containing 2μm plasmids with the *SLK1* gene (A), no DNA insert (B), the *NHP6A* gene (C), and the *NHP6B* gene (D). Transformants were grown at 24°C on IADE medium lacking uracil. The ability to rescue *slk1-1 spa2*-Δ lethality is indicated by dark (red) sectors and colonies due to loss of the p*SPA2/SUP4/CEN* plasmid.

which causes the cells to turn red on medium limiting for adenine. The p*SPA2/SUP4/CEN* plasmid contains a wild-type *SPA2* gene, which allows for growth of the *spa2*-Δ *slk1-1* strain, and *SUP4*, which suppresses the *ade2-101* mutation and thus prevents the formation of red pigment. This strain forms homogeneous white colonies (Fig. 1B), because the *SPA2* plasmid must be retained for viability. Strains containing a second plasmid that can complement either *slk1-1* or *spa2*-Δ will lose the p*SPA2/SUP4/CEN* plasmid at a high frequency and form white colonies with many red sectors. For example, a plasmid with the *SLK1* gene has this phenotype (Fig. 1A).

To identify genes that suppress *spa2*-Δ *slk1-1* lethality when present in high copy, a yeast genomic DNA library in a 2μm multicopy plasmid (9) was transformed into the starting strain, and transformants that are able to lose the p*SPA2/SUP4/CEN* plasmid were identified as white colonies with red sectors. Of 57,000 transformants, 52 plasmids that reproducibly allowed sectoring were identified (see Materials and Methods). Restriction mapping analysis indicated that 43 of these plasmids contained *SLK1*; none contained *SPA2*. The remaining 9 fell into four sequence classes (see Materials and Methods). One plasmid from each class was characterized further.

To determine whether the plasmids suppressed *spa2*-Δ, *slk1*-Δ, or both, the plasmids were transformed into three different strains: a *spa2*-Δ strain, a *spa2*-Δ *cdc10-10* strain containing p*SPA2/SUP4/CEN* (18), and a *slk1*-Δ strain. The *spa2*-Δ strain is defective in projection formation after pheromone treatment and has other polarity defects (20, 61). The *spa2*-Δ *cdc10-10* strain is not viable without the *SPA2/SUP4* plasmid. The *slk1*-Δ strain is temperature sensitive for growth and has other phenotypes (see below). One plasmid suppressed only *spa2*-Δ *cdc10-10* lethality and not *slk1*-Δ defects, suggesting that it specifically suppresses certain *spa2*-Δ defects. The other three plasmids suppressed the different defects of *slk1*-Δ (see below), but not the projection formation defects of *spa2*-Δ cells or the lethality of *spa2*-Δ *cdc10-10*. Sequence analysis of subclones containing the suppressing activity revealed that the *spa2*-Δ suppressor and two of the three *slk1*-Δ suppressors are previously unreported genes. Their characterization will be reported elsewhere.

The third *slk1*-Δ suppressor, which was isolated as two independent clones, was identical to the previously cloned gene, *NHP6A* (34). Multiple copies of a DNA fragment containing the full-length *NHP6A* ORF, 91 bp of upstream flanking DNA, and 129 bp of 3′ flanking DNA suppress the *spa2*-Δ *slk1-1* lethality (Fig. 1C) and *slk1*-Δ phenotypes (the temperature sensitivity and growth inhibition by low levels of caffeine, described below). Deletion of the 5′ flanking DNA and the first three codons of the *NHP6A* coding sequence abolished the ability of this suppressor to rescue the *slk1*-Δ mutant defects, confirming that suppression is due to the *NHP6A* gene. *S. cerevisiae* has a second gene, *NHP6B*, which is homologous to *NHP6A* (34). To determine whether multiple copies of *NHP6B* could also suppress *slk1*, a high-copy-number plasmid containing the *NHP6B* gene was transformed into *slk1-1* and *slk1*-Δ strains. The *NHP6B* multicopy plasmid was able to suppress the lethality of *spa2*-Δ *slk1-1* (Fig. 1D) and the phenotypes of the *slk1*-Δ mutation (data not shown). Thus, both *NHP6A* and *NHP6B* can suppress *slk1* defects.

Phenotypic analyses of *nhp6*-Δ mutants suggest that *NHP6* is important in some but not all of the same cellular processes as the *SLT2* pathway. Mutations in the *SLT2* pathway exhibit a variety of defects in growth control and morphogenesis. Deletion of *PKC1* results in lethality which is rescued by growth on osmotically stabilized medium (41, 48). Similarly, deletions of *SLK1*, *MKK* (*mkk1*-Δ *mkk2*-Δ cells), or *SLT2* result in a failure to form colonies at elevated temperatures (37°C) (11, 30, 38, 39, 46, 65) which can be suppressed by the addition of 1 M sorbitol to the medium (30, 38, 39, 46, 65). *slk1*-Δ and *slt2*-Δ cells have defects in shmoo formation and are sensitive to starvation (11, 12, 46). Furthermore, the growth of *slk1*-Δ cells and *slt2*-Δ cells is inhibited by low levels of caffeine in the medium (11) (see Fig. 5), and *slk1*-Δ and *slt2*-Δ mutants cannot grow at 30°C on medium containing glycerol as the primary carbon source (data not shown). Finally, both *slk1*-Δ and *slt2*-Δ are synthetically lethal with *spa2*-Δ cells, which is consistent with their participating in polarized growth and morphogenesis (11) (see Materials and Methods).

To analyze the in vivo functions of *NHP6A* and *NHP6B* and to determine whether these genes participate in the same cellular processes as *PKC1*, *SLK1*, and *SLT2*, several deletion and insertion mutations were made in each *NHP6* gene (described in Materials and Methods). Neither gene is essential, since *nhp6A*-Δ strains and *nhp6B*-Δ strains grow normally at all temperatures tested: 17, 24, 30, and 38°C. However, the *nhp6A*-Δ *nhp6B*-Δ double mutant strains grow normally at 24 and 30°C, grow poorly at 37°C, and fail to form colonies at 38°C (Fig. 2). The temperature-sensitive growth defect of *nhp6A*-Δ *nhp6B*-Δ cells is rescued by the addition of 1 M

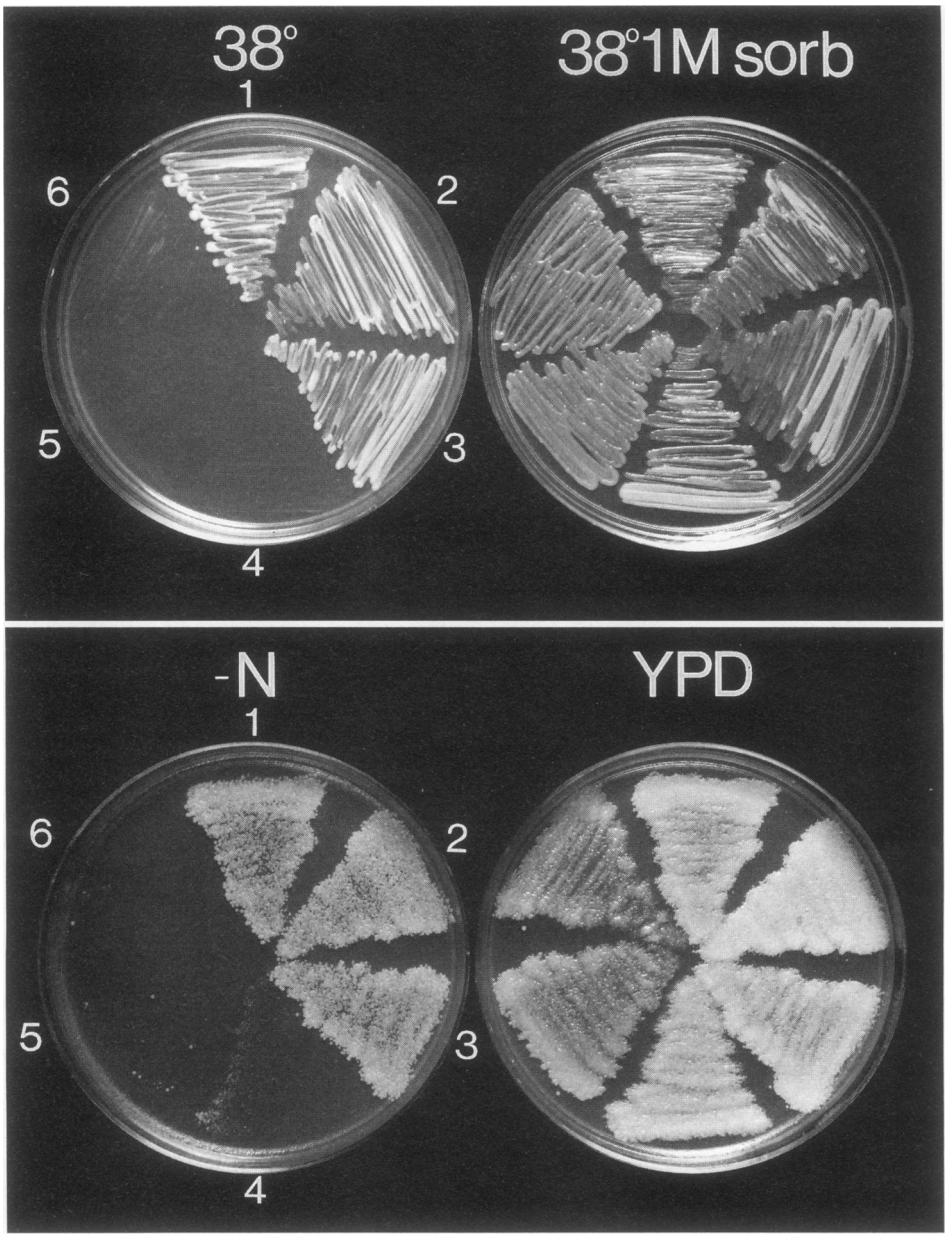

FIG. 2. Growth phenotypes of *nhp6*-Δ, *slk1*-Δ, and *slt2*-Δ mutants. Growth of the wild-type (1), *nhp6A*-Δ (2), *nhp6B*-Δ (3), *nhp6A*-Δ *nhp6B*-Δ (4), *slt2*-Δ (5), and *slk1*-Δ (6) strains is shown. (Top row left): *slk1*-Δ, *slt2*-Δ, and *nhp6A*-Δ *nhp6B*-Δ mutants fail to grow on YPD plates at 38°C; (top row right) the growth defect at 38°C is rescued by the addition of 1 M sorbitol (sorb) to the medium. (Bottom row) Nitrogen starvation sensitivity of *slk1*-Δ, *slt2*-Δ, and *nhp6A*-Δ *nhp6B*-Δ strains. (Left) Cells were grown on YPD plates for 3 days, transferred to yeast minimal medium lacking nitrogen (YM-N) plates at 30°C for 7 days, and then transferred to YPD plates and grown for 3 days. (Right) Control replica plates of nonstarved cells were incubated at 30°C on YPD medium after growth on YPD medium for 3 days at 30°C.

sorbitol to the medium (Fig. 2), as observed for *slk1*-Δ and *slt2*-Δ mutants. Quantitative growth rate measurements demonstrate that this osmoremediation restores growth at 38°C to 37% of wild-type rates.

The *nhp6* mutants were also tested for their ability to survive nitrogen starvation. *nhp6A*-Δ and *nhp6B*-Δ strains were not sensitive, whereas the *nhp6A*-Δ *nhp6B*-Δ double mutants were sensitive to nitrogen starvation (Fig. 2). Wild-type, *nhp6A*-Δ, and *nhp6B*-Δ cells recover after incubation for 1 week on medium lacking nitrogen (YM-N) and then by transfer to rich medium; however, *nhp6A*-Δ *nhp6B*-Δ strains are severely impaired in recovery. These results suggest that *NHP6A* and *NHP6B* are functionally redundant, since only the double mutant has an observable phenotype and since either gene on a high-copy-number plasmid can suppress *slk1*-Δ defects. Importantly, the results also indicate that cells lacking *NHP6* function have many mutant phenotypes similar to those reported for mutants in the *SLT2* pathway.

However, *nhp6A*-Δ *nhp6B*-Δ mutants do not exhibit all of the mutant phenotypes of *slk1*-Δ and *slt2*-Δ cells, and/or the *nhp6A*-Δ *nhp6B*Δ mutant phenotypes appear less severe. Unlike *SLT2* pathway mutants, *nhp6A*-Δ *nhp6B*-Δ mutants are not

inhibited for growth in the presence of caffeine (concentrations of up to 11 mM tested) at 30°C and are able to grow on medium containing glycerol as the primary carbon source at 30 and 37°C (data not shown). *nhp6A*-Δ *nhp6B*-Δ cells form normal mating projections and the *nhp6*-Δ mutations are not lethal in a *spa2*-Δ background. Sporulation of a *MAT***a**/*MAT*α *spa2*-Δ/*SPA2 nhp6A*-Δ/*NHP6A nhp6B*-Δ/*NHP6B* diploid and analysis of 30 tetrads revealed that 13% of the segregants were *spa2*-Δ *nhp6A*-Δ *nhp6B*-Δ, approximately the number of such segregants that is expected under the assumption of Mendelian segregation. Thus, *nhp6*-Δ cells have many characteristics of *slt2*-Δ and *slk1*-Δ mutant cells yet are normal in other respects.

***nhp6A*-Δ *nhp6B*-Δ mutants have morphological defects.** In addition to the growth defects described above, *SLT2* pathway mutants have a variety of morphological defects. These include rapid lysis after shift to nonpermissive growth conditions (38, 39, 46, 65), aberrant neck and bud formation (11, 48), and the formation of long chains of cells (48). Since the *nhp6* double mutants have many growth defects similar to those of *slk1*-Δ, *slt2*-Δ, and *pkc1*-Δ mutants, the *nhp6A*-Δ *nhp6B*-Δ cells were examined for morphological defects by light and scanning electron microscopic techniques.

In liquid medium, *nhp6A*-Δ *nhp6B*-Δ mutants ceased growth after ~12 h at the restrictive temperature, 38°C, and after prolonged incubation (greater than 28 h), the cells appeared nonrefractile in the light microscope, which is suggestive of cell lysis (data not shown). This phenotype is also observed in *SLT2* pathway mutants incubated at the nonpermissive temperature, except that the lysis occurs much more rapidly for *slk1*-Δ and *slt2*-Δ mutants. Incubation of *nhp6A*-Δ *nhp6B*-Δ mutant cells at 38°C leads to an accumulation of cells with enlarged necks and a high proportion of connected cells (Fig. 3B). After 22 h at 38°C, 15% of *nhp6A*-Δ *nhp6B*-Δ mutants had enlarged necks (n = 310 cells counted) and 7% of *nhp6A*-Δ *nhp6B*-Δ mutant cells were in chains composed of three or more cells (n = 375 cells counted). A subset of cells (10%) with enlarged necks also had elongated buds. By comparison, <1% of wild-type cells (n = 368) had enlarged necks or chains of three or more cells. *nhp6A*-Δ *nhp6B*-Δ cells shifted to the restrictive temperature are often larger than similarly treated wild-type cells and have irregular shapes (Fig. 3B). Staining of DNA with Hoechst stain showed that 97% (at 22 h [n = 430]) of all cells contained a single nucleus, indicating that there is no defect in nuclear division. The osmoremediation of *nhp6A*-Δ *nhp6B*-Δ temperature-sensitive growth did not alleviate the morphological defects; at 22 h, 16% of *nhp6A*-Δ *nhp6B*-Δ cells incubated in YPD medium containing 1 M sorbitol had aberrant morphologies (n = 318).

The *nhp6A*-Δ *nhp6B*-Δ cell population at 38°C was also analyzed by scanning electron microscopy (Fig. 3D). The observations were consistent with those obtained by light microscopy; the necks of *nhp6A*-Δ *nhp6B*-Δ mutants were often enlarged at cytokinesis, the double-mutant cells were often bigger than the wild-type cells, and chains of cells were frequently observed. Thus, in general, the morphological defects of *nhp6A*-Δ *nhp6B*-Δ cells are similar to but less severe than those of *slk1*-Δ and *slt2*-Δ mutants at 37°C. Some features of *nhp6A*-Δ *nhp6B*-Δ mutants are also reminiscent of those described for *pkc1*-Δ mutants (see Discussion).

***nhp6A*-Δ *nhp6B*-Δ mutants have altered distributions of chitin and actin.** *slt2*-Δ cells grown at the restrictive temperature in 1 M sorbitol have polarity defects; these cells contain partially delocalized actin distributions and accumulate secretory vesicles (46). Because *nhp6* mutants have many of the same morphological defects as mutants in the *SLT2* pathway, we analyzed the distribution of two components of polarized growth, chitin, and actin, in *nhp6A*-Δ *nhp6B*-Δ strains. In wild-type cells, chitin is primarily deposited at the neck between the mother and daughter cells. After cell separation, it remains on the mother cell and can be detected by Calcofluor labelling as a circular bud scar; the daughter birth scar is not labelled (44, 45, 60). Lower levels of chitin are also accumulated throughout the cell wall and are readily detectable in older cells. Typically, mother cells exhibit low-level Calcofluor labelling of the cell wall, while daughter cells stain more weakly (Fig. 4A). Delocalized chitin deposition is a hallmark of yeast mutants with defects in polarized growth. Among such mutants are *act1*, *pfy1*, *cap2*, *cdc24*, and *myo2*, which have diffuse patches of chitin spread discontinuously over the surfaces of mother cells and little chitin on daughter cell surfaces (see references in reference 44).

Staining with Calcofluor reveals that *nhp6A*-Δ *nhp6B*-Δ mutants have a novel defect in chitin deposition (Fig. 4B). After 22 h at 38°C, 35% of *nhp6A*-Δ *nhp6B*-Δ cells (n = 314) had aberrant chitin deposition; chitin patches and/or enhanced chitin deposition at the neck at cytokinesis was observed (defined further in Materials and Methods). Wild-type cells lacked these patches (n = 367). Addition of 1 M sorbitol to the medium partially alleviated the chitin deposition defect of *nhp6A*-Δ *nhp6B*-Δ cells. At 22 h, 24% of *nhp6A*-Δ *nhp6B*-Δ cells incubated in YPD medium containing 1 M sorbitol had aberrant Calcofluor staining (n = 343). Similarly treated *slt2*-Δ cells did not display the observed defect in chitin deposition, indicating that this defect is specific for *nhp6A*-Δ *nhp6B*-Δ mutant strains. The increase in aberrant chitin patches after prolonged incubation at 38°C correlated with a small decrease in cells with normal, circular bud scars, although the decrease in bud scars was not as dramatic as the increase in chitin patches. After the shift to 38°C, the percentage of cells with chitin patches increased from 0 to 31%; the frequency of cells with bud scars decreased from 24 to 12%. This suggests that a subset of the chitin patches in *nhp6A*-Δ *nhp6B*-Δ mutants might be defective bud scars.

Bud scars were also examined in wild-type cells and in *nhp6A*-Δ *nhp6B*-Δ cells by scanning electron microscopy. As was observed by Calcofluor staining, bud scars were significantly depleted in the *nhp6A*-Δ *nhp6B*-Δ mutant population. After 14 h at 38°C, 5% of *nhp6A*-Δ *nhp6B*-Δ cells had detectable bud scars (n = 410), compared with 37% of wild-type cells (n = 426). No structures which might be candidates for defective bud scars were detected on the surfaces of the *nhp6A*-Δ *nhp6B*-Δ cells.

The actin cytoskeleton is also abnormal in *nhp6A*-Δ *nhp6B*-Δ mutants at the restrictive temperature (Fig. 4D). Wild-type cells growing exponentially at 38°C accumulate actin spots in a ring at the incipient bud site in unbudded cells and at the cell cortex of the bud in budded cells (1, 44, 45) (Fig. 4C). In contrast, after 9 h at 38°C, 15% of *nhp6A*-Δ *nhp6B*-Δ mutant cells contained actin spots uniformly distributed in both the mother cell and bud (n = 351 cells), similar to the results described for *slt2*-Δ cells (46). In addition, a significant fraction of *nhp6A*-Δ *nhp6B*-Δ mutants (24 and 31%, at 9 and 18.5 h, respectively; n [9 h] = 351; n [18.5 h] = 389) contain large actin chunks (defined in Materials and Methods and shown in Fig. 4D). Double labelling experiments with Calcofluor and rhodamine-phalloidin demonstrated that actin chunks and chitin patches do not colocalize (data not shown). The presence of 1 M sorbitol partially alleviates the loss of actin polarity (11% of cells have delocalized actin after 9 h at 38°C [n = 318]), and chunks are still visible (22% after 9 h [n = 318]). *slt2*-Δ mutants grown in the presence of sorbitol at the restrictive temperature also have disrupted actin polarity. Thus, in summary, both

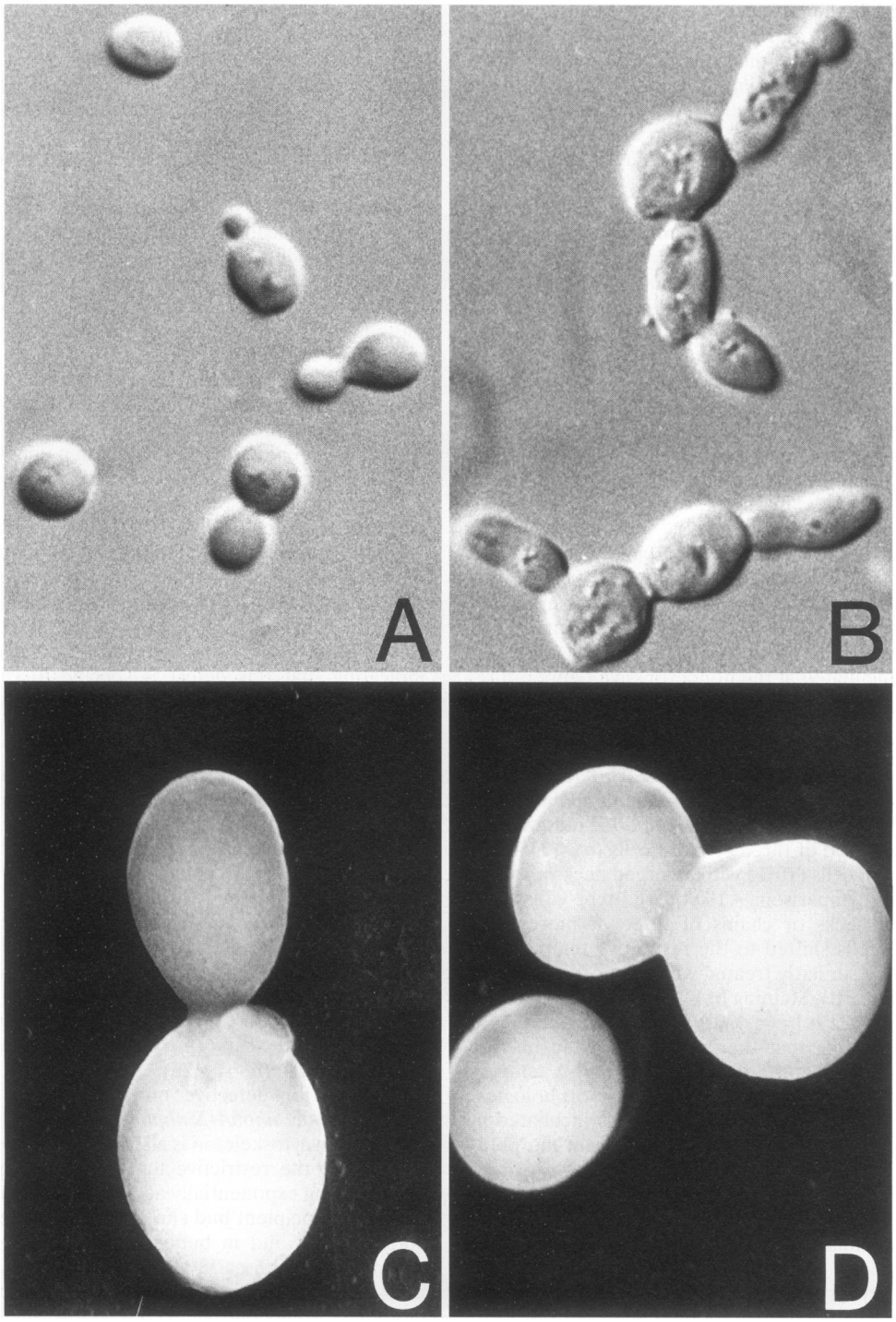

FIG. 3. *nhp6A*-Δ *nhp6B*-Δ cells often exhibit morphological defects including elongated buds, long chains of cells, and enlarged necks. Morphology of wild-type (A) and *nhp6A*-Δ *nhp6B*-Δ (B) cells by differential-interference contrast microscopy after incubation at 38°C for 11.5 h (magnification, ×1,000) and of wild-type (C) and *nhp6A*-Δ *nhp6B*-Δ (D) cells by scanning electron microscopy after incubation at 38°C for 14 h (magnification, ×9,840) is shown. A bud scar near the neck of the wild-type cell is shown in panel C.

actin and chitin distribution in the *nhp6A*-Δ *nhp6B*-Δ mutant strain are disrupted.

Genetic evidence suggests that *NHP6* functions in the *SLT2* MAPK pathway. The phenotypes of the *nhp6A*-Δ *nhp6B*-Δ mutants and the suppression of *slk1*-Δ by multiple copies of *NHP6* suggested that these genes might operate in the same pathway. This possibility was examined by genetic tests. If Nhp6p is a downstream component of the Slt2p pathway and is involved in functions controlled by that pathway, *slk1*-Δ is expected to be epistatic to *nhp6A*-Δ *nhp6B*-Δ; if Nhp6p operates in a pathway parallel to the Slt2p pathway, then *slk1*-Δ is expected to enhance *nhp6A*-Δ *nhp6B*-Δ mutant defects and

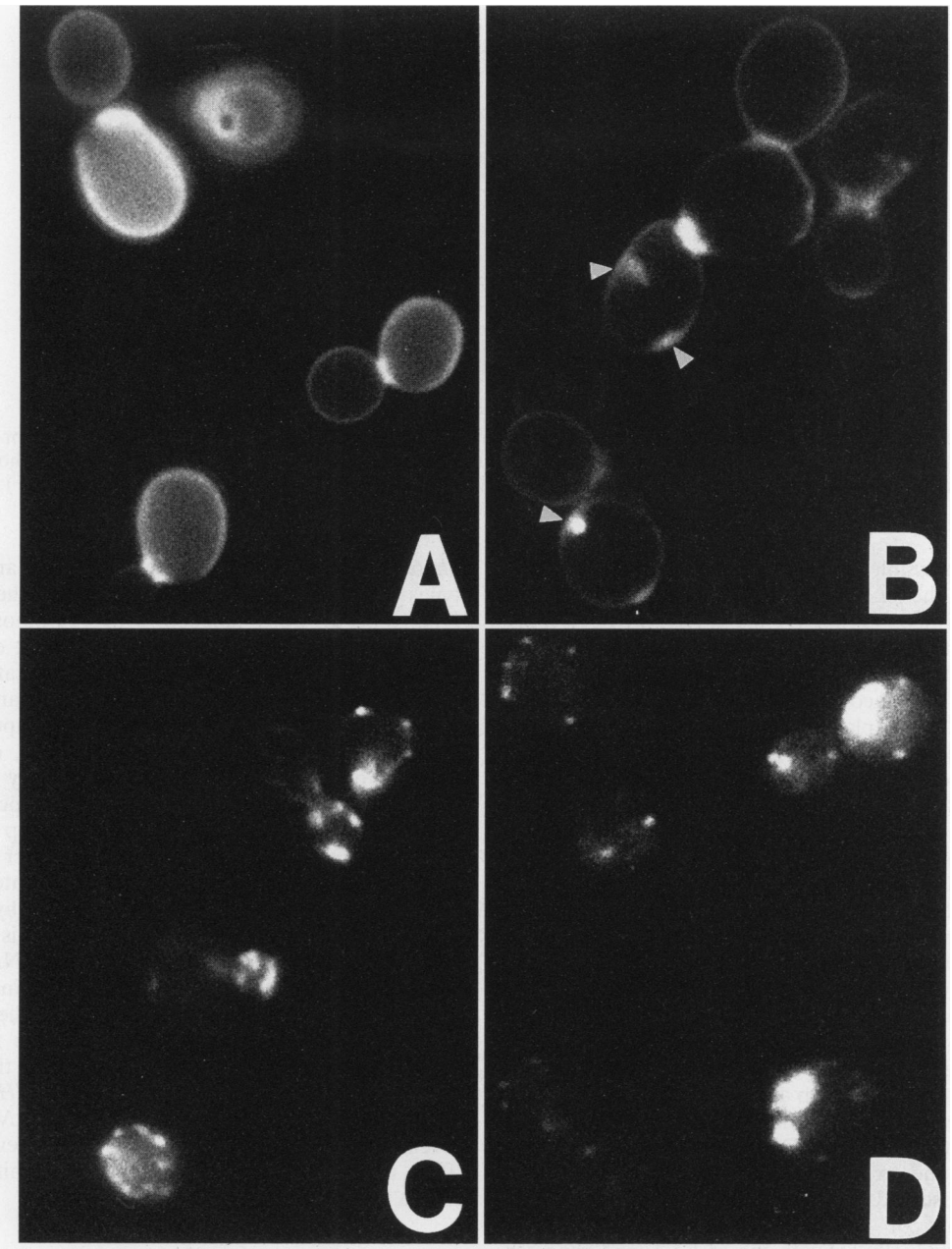

FIG. 4. *nhp6A*-Δ *nhp6B*-Δ cells have defects in chitin and actin distribution. Wild-type (A and C) and *nhp6A*-Δ *nhp6B*-Δ (B and D) cells were fixed after incubation at 38°C for 11.5 h and were stained with either Calcofluor (A and B) or rhodamine-phalloidin (C and D). The wild-type cell shown in the upper left-hand corner (A) contains a bud scar which is out of the plane of focus and stains brightly with Calcofluor; arrowheads (B) point to chitin patches.

perhaps even to cause inviability. These possibilities were tested by analyzing *slk1*-Δ *nhp6A*-Δ *nhp6B*-Δ segregants of a *MAT***a**/α *slk1*-Δ/*SLK1 nhp6A*-Δ/*NHP6A nhp6B*-Δ/*NHP6B* diploid. Of 44 tetrads that were dissected and germinated at 24°C, 17 segregants (11% of the viable segregants) were *nhp6A*-Δ *nhp6B*-Δ *slk1*-Δ, 14 segregants (9%) were *nhp6A*-Δ *nhp6B*-Δ, and 13 segregants (8%) were *slk1*-Δ. Thus, there is no increase in inviability of the triple mutants compared with that of *slk1*-Δ or *nhp6A*-Δ *nhp6B*-Δ alone. Analysis of colony growth at 30 and 32°C (a semipermissive temperature for *slk1*-Δ) revealed that the *nhp6A*-Δ *nhp6B*-Δ *slk1*-Δ mutants grew as well as the *slk1*-Δ mutants. As expected, the *nhp6A*-Δ *nhp6B*-Δ *slk1*-Δ cells failed to grow at 38°C, and this growth defect was rescued when the medium was osmotically stabilized by 1 M sorbitol. Thus, since the presence of the *nhp6A*-Δ *nhp6B*-Δ mutations did not enhance the defects of *slk1*-Δ, it appears that Nhp6p operates in the same pathway as Slk1p.

Similarly, we used high-copy-number suppression tests to determine whether *NHP6A* and *NHP6B* operate upstream or downstream of *SLT2*. As shown in Fig. 5, multiple copies of either *NHP6* gene suppress the temperature-sensitive growth defect of *slt2*-Δ cells and the inhibition of growth by caffeine. The failure of *slt2*-Δ cells to grow on the nonfermentable carbon source, glycerol, and the *slt2*-Δ starvation sensitivity

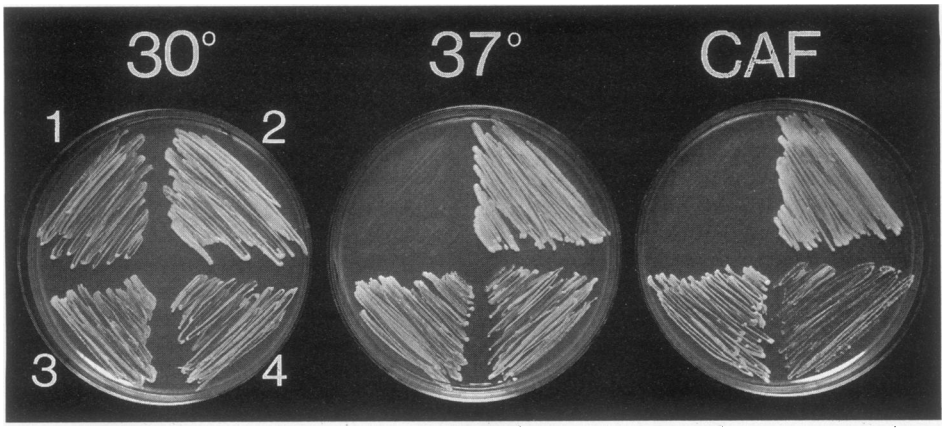

FIG. 5. Multiple copies of the *NHP6A* and *NHP6B* genes suppress *slt2*-Δ defects. *slt2*-Δ cells containing either a 2μm vector (1), the *SLT2* gene on a *CEN* plasmid (2), the 2μm plasmid carrying the *NHP6A* gene (3), or the 2μm plasmid carrying the *NHP6B* gene (4) are shown. Transformants were grown on media lacking uracil at 30°C (left) or 37°C (middle) or at 30°C on medium containing 3 mM caffeine (CAF) (right).

were weakly suppressible by both *NHP6* genes (data not shown). However, the *slt2*-Δ defect in shmoo formation was not suppressible. Thus, multiple copies of *NHP6A* or *NHP6B* suppress many, but not all, of the defects of *slt2*-Δ cells.

Finally, we also tested whether multicopy plasmids carrying *PKC1*, *SLK1*, or *SLT2* could suppress *nhp6A*-Δ *nhp6B*-Δ mutants. None of these plasmids rescued the temperature-sensitive growth defect of *nhp6A*-Δ *nhp6B*-Δ mutants (data not shown). Thus, these different genetic tests indicate that Nhp6p functions in the same pathway as Slk1p and Slt2p and that Nhp6p operates downstream of Slt2p and the other known genes in the pathway.

The Slt2 MAPK and the Nhp6A proteins do not appear to interact in vivo. Genetic and phenotypic analysis suggests that Nhp6p is a downstream component of the Slt2p MAPK pathway. One possibility is that Nhp6p is a substrate of the Slt2p MAPK pathway. The possible interaction of Slt2p and Nhp6Ap in vivo was tested by using the yeast two-hybrid system (17). In a variation of the system originally developed by Fields and Song (17), one protein is fused to the transcriptional activation domain of Gal4p and the other is fused to the DNA-binding domain of LexA. If the two proteins interact, the transcriptional activation and DNA-binding domains are brought together and expression of a LexA-inducible *lacZ* reporter gene is observed.

First, the ability of LexA::Slt2p, LexA::Nhp6Ap, and Gal4::Slt2p to individually activate the *pLEXA-lacZ* reporter gene was tested. The LexA::Slt2p fusion protein strongly activated expression of β-galactosidase, while the LexA::Nhp6Ap and Gal4::Slt2p fusions did not yield detectable levels of expression (data not shown). This suggests that Slt2p serves to help activate transcription in this assay and that Nhp6Ap does not. Introduction of p*GAL4*::*SLT2* into a strain carrying p*LexA*::*NHP6A* did not induce expression of the reporter gene. This result suggests that Slt2p and Nhp6Ap do not interact in vivo. However, the strength of this conclusion is moderated by the inability to prove that the LexA::Nhp6Ap fusion protein was able to bind to the reporter gene promoter and by the possibility that the two proteins interact only weakly and thus may not produce a positive result in this assay.

We also searched for in vivo phosphorylation of Nhp6Ap using ^{32}P-labelling experiments. An HA epitope was introduced at the N-terminal coding sequences of *NHP6A* on a high-copy-number plasmid; the resulting HA::Nhp6Ap appeared to be functional, since this plasmid complemented *nhp6A*-Δ *nhp6B*-Δ and suppressed *slk1*-Δ and *slt2*-Δ phenotypes (data not shown). Cells carrying the epitope-tagged HA::Nhp6Ap were labelled with [^{32}P]phosphate, and the protein was immunoprecipitated from cell extracts by using anti-HA antibodies. The immunoprecipitated protein was readily detected by probing gel blots with anti-HA; however, autoradiography revealed that the HA::Nhp6Ap was not detectably phosphorylated (data not shown), even though ^{32}P labelling of total cellular protein was readily apparent in total cell lysates. Thus, both the two-hybrid experiments and the ^{32}P-labelling experiments suggest that Nhp6p is not a substrate for Slt2p. However, the possibilities of either weak interaction and/or transient labelling cannot be eliminated.

***NHP6* is not transcriptionally regulated by the *SLT2* pathway.** To address the possibility that *NHP6* is transcriptionally regulated by the *SLT2* pathway, *NHP6* RNA levels in wild-type, *slk1*-Δ, and *slt2*-Δ strains were examined by RNA blot analysis (data not shown). *NHP6A* RNA is the major transcript of the *NHP6* genes in vivo (33) and was readily detected; *NHP6B* RNA was not detected in any of the strains in our experiments. Quantitative comparison of *NHP6A* RNA levels in *slk1*-Δ and *slt2*-Δ strains revealed that *NHP6A* transcript levels were 82 and 98% of the wild-type levels, respectively. Thus, the levels of *NHP6A* RNA are not significantly altered in *slk1*-Δ and *slt2*-Δ strains.

DISCUSSION

Nhp6Ap and Nhp6Bp function in the Slt2p MAPK pathway. In this study, a synthetic lethal suppression screen was used to identify downstream components of the Slt2p MAPK pathway. Nhp6Ap and Nhp6Bp are functionally redundant proteins, and strains with mutations in the *NHP6A* and *NHP6B* genes have many similarities to those with mutations in the *SLT2* pathway (summarized in Table 2): failure to grow at high temperatures and cell lysis, rescue of growth defects by 1 M sorbitol, starvation sensitivity, loss of actin polarity at 38°C, and morphological defects (e.g., chains of connected cells and elongated buds; see below). Analysis of triple mutants (*slk1*-Δ *nhp6A*-Δ *nhp6B*-Δ) indicates that *NHP6A* and *NHP6B* operate in the *SLT2* pathway, and multicopy suppression experiments suggest that Nhp6p function lies downstream of Slt2p. On the basis of these data, we propose the schemes shown in Fig. 6. In these models, Nhp6Ap and Nhp6Bp compose one branch in the pathway downstream of Slt2p. Certain morphological traits

TABLE 2. Summary of genetic interactions and phenotypes of *SLT2* pathway mutants[a]

Mutant strain	Presence of the following genetic interactions[b]			Presence of the following phenotypes					
	Multicopy *NHP6* suppression	Multicopy *SLT2* suppression	Viability with *spa2*-Δ	Growth at 38°C	Growth at 38°C + 1 M sorbitol	Survival after N starvation	Actin distribution	Growth on glycerol[c]	Caffeine resistance[c,d]
slk1-Δ	+	+	−	−	+	−	Not tested	−	−
slt2-Δ	+	+	−	−	+	−	Abnormal	−	−
nhp6-Δ	+	−	+	−	+	−/+	Abnormal	+	+
Wild type	NA	NA	+	+	+	+	Normal	+	+

[a] Phenotypes were tested as described in the text.
[b] For *nhp6*-Δ, only temperature-sensitive growth defects were tested for suppression. For *slk1*-Δ, temperature-sensitive growth defects and caffeine sensitivity were examined. For *slt2*-Δ temperature-sensitive growth defects, caffeine sensitivity, glycerol growth defects, and nitrogen starvation sensitivity defects were examined. +, all of the tested defects were suppressed. NA, not applicable.
[c] Tested at 30°C.
[d] An 11 mM concentration of caffeine was used.

and specific functions that allow growth at higher temperatures and survival of starvation depend on Nhp6Ap and Nhp6Bp.

Since the phenotypes of *nhp6A*-Δ *nhp6B*-Δ mutant cells are not as severe as those of *slk1*-Δ or *slt2*-Δ cells, we speculate that an *NHP6*-independent branch exists in the *SLT2* pathway. Unlike *slk1*-Δ and *slt2*-Δ mutants, the *nhp6A*-Δ *nhp6B*-Δ cells grow slightly at 37°C and do not arrest (or lyse) immediately after a shift to their restrictive temperature of 38°C. Furthermore, *nhp6A*-Δ *nhp6B*-Δ cells, unlike *slk1*-Δ and *slt2*-Δ cells, can grow on glycerol medium, are not inhibited for growth by caffeine, and do not have a shmoo formation defect. We hypothesize that the non-*NHP6* growth defects are due either to Slt2p phosphorylation of multiple substrates (Fig. 6A) or to Slt2p phosphorylation of a common substrate that has some *NHP6*-dependent activities and a different set of *NHP6*-independent activities (Fig. 6B).

The data presented here indicate that Nhp6p functions downstream of the Slt2p MAPK. Slt2p and Nhp6Ap do not appear to be in a direct kinase-substrate relationship, since they did not interact in vivo by the two-hybrid system and [^{32}P]phosphate-labelling experiments indicated that Nhp6Ap is not stably phosphorylated in vivo. Furthermore, although two potential MAPK phosphorylation sites (X-S/T-P [where X is any residue; 3, 50]) are present in Nhp6Ap (amino acid residues 2 to 4 and 62 to 64), no such sites are present in Nhp6Bp. Since Nhp6Ap and Nhp6Bp are functionally redundant, phosphorylation at the predicted MAPK consensus phosphorylation site cannot be essential for function of Nhp6p. Thus, it is more likely that these proteins either work with an Slt2p substrate or function downstream of the substrate.

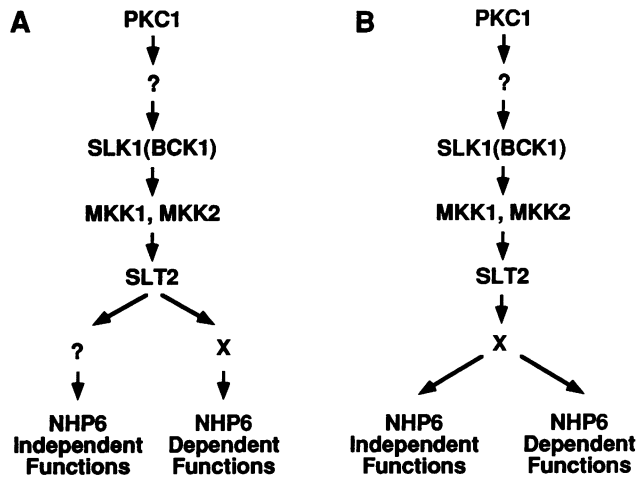

FIG. 6. Possible models for Nhp6p function downstream in the Slt2p pathway. See text for details. Component X might function directly with Nhp6p or upstream of Nhp6p.

HMG1s have been shown to be associated with transcriptionally active chromatin (31, 42) and appear to facilitate formation of transcription initiation complexes (66). Nhp6p is a DNA-binding protein (33) whose possible role in transcription regulation is being investigated. One possibility is that Nhp6p acts in conjunction with a transcription factor(s) that is a substrate of Slt2p. This transcription factor might require Nhp6p function to activate expression at some promoters, but the transcription factor could activate without Nhp6p at other promoters. This would yield the *NHP6*-dependent and *NHP6*-independent functions observed downstream in the *SLT2* pathway.

When present in a high-copy-number plasmid, either NHP6 gene can suppress the caffeine sensitivity of *slk1*-Δ and *slt2*-Δ cells and can weakly suppress the glycerol growth defect. However, the *nhp6A*-Δ *nhp6B*-Δ mutants themselves are not caffeine sensitive and can grow on glycerol medium. One possibility is that there is a third gene with some NHP6-like function which prevents *nhp6A*-Δ *nhp6B*-Δ cells from acquiring the caffeine and glycerol growth defects. An alternative explanation is that loss of NHP6 function only partially cripples a putative Slt2p substrate that works with Nhp6p. Loss of Nhp6 function would allow some activity of the substrate and allow growth in the presence of caffeine or on glycerol medium. Overexpression of *NHP6* could increase the activity of the Slt2 substrate and thereby suppress the growth defects. Characterization of additional components of the *SLT2* pathway will help distinguish among these different possibilities.

Some morphological defects of *nhp6A*-Δ *nhp6B*-Δ cells are similar to those of *SLT2* pathway mutants, while others are different. Many of the morphological defects of *nhp6A*-Δ *nhp6B*-Δ cells are similar to those described for *SLT2* pathway mutants. The chains of connected cells and elongated buds of *nhp6A*-Δ *nhp6B*-Δ cells are remarkably similar to those of *pkc1*-Δ mutants grown on osmostabilized solid medium (compare Fig. 3 with Fig. 8 of Paravicini et al. [48]). Failure in proper constriction at the neck is found for *slk1* mutants (11) and is suggested in *pkc1*-Δ cells by transmission electron microscopy, which clearly shows the failure to form a septum between cells in a chain (48). Finally, actin polarity is disrupted

in *nhp6A*-Δ *nhp6B*-Δ mutants in a manner similar to that described for *slt2*-Δ cells (46).

Some of the *nhp6A*-Δ *nhp6B*-Δ phenotypes are novel. Chitin patches and actin chunks are visible in *nhp6*-Δ cells and are not evident in *SLT2* pathway mutants. Since *nhp6A*-Δ *nhp6B*-Δ cells have less severe defects than *SLT2* pathway mutants, we speculate that these aberrant structures and other morphological defects result from a more subtle but similar underlying cytoskeletal defect that is present in *SLT2* pathway mutants. In *slt2*-Δ mutants, lysis ensues quickly (within 4 h [38, 46, 65]). For *nhp6A*-Δ *nhp6B*-Δ strains, lysis is comparatively delayed (nonrefractile cells become obvious after 28 h) and is preceded by the cytoskeletal and chitin deposition anomalies.

To our knowledge, no mutant that contains the aberrant chitin patches has been described previously. It is possible that some of these are the product of a cytokinesis defect. The presence of connected cells and enhanced staining at the neck is consistent with such a defect. Unlike the chitin patches, phalloidin-stained actin chunks have been recently observed. Holtzman et al. (29) observed actin chunks in *sla1*-Δ mutants (which are synthetically lethal with a mutation in the *ABP1* gene, which encodes an actin-binding protein). Actin chunks are a clear indicator of a defect in the actin cytoskeleton. A potential underlying defect of all *SLT2* pathway mutants is a defect in the cytoskeleton and/or polarized secretion (11, 46). Such defects could result in a loss of polarized deposition of the cell wall components, thereby causing cell lysis.

In summary, the synthetic lethal suppression screen described above has identified a putative component of the Slt2p MAPK pathway. Further analysis of the other suppressor clones may yield insights into polarity and morphogenesis in yeast cells. Synthetic lethal suppression is expected to be a generally useful approach for identifying genes that operate in pathways of interest.

ACKNOWLEDGMENTS

We thank K. Madden and L. Vallier for comments on the manuscript and M. Tibbetts and D. Stern for useful suggestions.

This research was supported by NIH grants GM36494 to M.S. and GM45793 to D.K. C.C. was partially supported by a John Woodruff Simpson Fellowship award.

REFERENCES

1. **Adams, A. E., and J. R. Pringle.** 1984. Relationship of actin and tubulin distribution to bud growth in wild-type and morphogenetic-mutant *Saccharomyces cerevisiae*. J. Cell Biol. **98:**934–945.
2. **Ahn, N. G., R. Seger, and E. G. Krebs.** 1992. The mitogen-activated protein kinase activator. Curr. Opin. Cell Biol. **4:**992–999.
3. **Alvarez, E., I. C. Northwood, F. A. Gonzalez, D. A. Latour, A. Seth, C. Abate, T. Curran, and R. J. Davis.** 1991. Pro-Leu-Ser/Thr-Pro is a consensus primary sequence for substrate protein phosphorylation. J. Biol. Chem. **266:**15277–15285.
4. **Barrett, J., and M. Snyder.** Unpublished data.
5. **Blenis, J.** 1993. Signal transduction via the MAP kinases: proceed at your own RSK. Proc. Natl. Acad. Sci. USA **90:**5889–5892.
6. **Boeke, J., J. Trueheart, G. Natsoulis, and G. R. Fink.** 1987. 5-Fluoroorotic acid as a selective agent in yeast molecular genetics. Methods Enzymol. **154:**164–175.
7. **Botstein, D., S. C. Falco, S. E. Stewart, M. Brennan, S. Scherer, D. T. Stinchcomb, K. Struhl, and R. W. Davis.** 1979. Sterile host yeasts (SHY): a eukaryotic system of biological containment for recombinant DNA experiments. Gene **8:**17–24.
8. **Brewster, J. L., T. de Valoir, N. D. Dwyer, E. Winter, and M. C. Gustin.** 1993. An osmosensing signal transduction pathway in yeast. Science **259:**1760–1763.
9. **Carlson, M., and D. Botstein.** 1982. Two differentially regulated mRNAs with different 5′ ends encode secreted and intracellular forms of yeast invertase. Cell **28:**145–154.
10. **Chen, R.-H., C. Sarnecki, and J. Blenis.** 1992. Nuclear localization and regulation of *erk*- and *rsk*-encoded protein kinases. Mol. Cell. Biol. **12:**915–927.
11. **Costigan, C., S. Gehrung, and M. Snyder.** 1992. A synthetic lethal screen identifies SLK1, a novel protein kinase homolog implicated in yeast cell morphogenesis and cell growth. Mol. Cell. Biol. **12:**1162–1178.
12. **Costigan, C., and M. Snyder.** SLK1, a yeast homolog of MAP kinase activators, has a RAS/cAMP-independent role in nutrient sensing. Mol. Gen. Genet., in press.
13. **Courchesne, W. E., R. Kunisawa, and J. Thorner.** 1989. A putative protein kinase overcomes pheromone-induced arrest of cell cycling in *S. cerevisiae*. Cell **58:**1107–1119.
14. **Dent, P., W. Haser, T. A. Haystead, L. A. Vincent, T. M. Roberts, and T. W. Sturgill.** 1992. Activation of mitogen-activated protein kinase kinase by v-Raf in NIH 3T3 cells and in vitro. Science **257:**1404–1407.
15. **Elion, E. A., P. L. Grisafi, and G. R. Fink.** 1990. *FUS3* encodes a cdc2+/CDC28-related kinase required for the transition from mitosis into conjugation. Cell **60:**649–664.
16. **Engebrecht, J., J. Hirsch, and G. S. Roeder.** 1990. Meiotic gene conversion and crossing over: their relationship to each other and to chromosome synapsis and segregation. Cell **62:**927–937.
17. **Fields, S., and O.-K. Song.** 1989. A novel genetic system to detect protein-protein interactions. Nature (London) **340:**245–246.

17a. **Fields, S., and R. Sternglanz.** Unpublished data.

18. **Flescher, E. G., K. Madden, and M. Snyder.** 1993. Components required for cytokinesis are important for bud site selection in yeast. J. Cell Biol. **122:**373–386.
19. **Gartner, A., K. Nasmyth, and G. Ammerer.** 1992. Signal transduction in *Saccharomyces cerevisiae* requires tyrosine and threonine phosphorylation of FUS3 and KSS1. Genes Dev. **6:**1280–1292.
20. **Gehrung, S., and M. Snyder.** 1990. The *SPA2* gene of *Saccharomyces cerevisiae* is important for pheromone-induced morphogenesis and efficient mating. J. Cell Biol. **111:**1451–1464.
21. **Gille, H., A. D. Sharrocks, and P. E. Shaw.** 1992. Phosphorylation of transcription factor $p62^{TCF}$ by MAP kinase stimulates ternary complex formation at c-*fos* promoter. Nature (London) **358:**414–417.
22. **Gimeno, C. J., P. O. Ljungdahl, C. A. Styles, and G. R. Fink.** 1992. Unipolar cell divisions in the yeast *S. cerevisiae* lead to filamentous growth: regulation by starvation and *RAS*. Cell **68:**1077–1090.
23. **Golemis, E. A., and R. Brent.** 1992. Fused protein domains inhibit DNA binding by LexA. Mol. Cell. Biol. **12:**3006–3014.
24. **Gomez, N., and P. Cohen.** 1991. Dissection of the protein kinase cascade by which nerve growth factor activates MAP kinases. Nature (London) **353:**170–173.

24a. **Hanes, S., and R. Brent.** Unpublished data.

25. **Harlow, E., and D. Lane.** 1988. Antibodies: a laboratory manual. Cold Spring Harbor Laboratory, Cold Spring Harbor, N.Y.
26. **Haycock, J. W., N. G. Ahn, M. H. Cobb, and E. G. Krebs.** 1992. ERK1 and ERK2, two microtubule-associated protein 2 kinases, mediate the phosphorylation of tyrosine hydroxylase at serine-31 *in situ*. Proc. Natl. Acad. Sci. USA **89:**2365–2369.
27. **Henikoff, S.** 1987. Unidirectional digestion with exonuclease III in DNA sequence analysis. Methods Enzymol. **155:**156–165.
28. **Hill, J. E., A. M. Myers, T. J. Koerner, and A. Tzagoloff.** 1986. Yeast/*E. coli* shuttle vectors with multiple unique restriction sites. Yeast **2:**163–167.
29. **Holtzman, D., S. Yang, and D. Drubin.** 1993. Synthetic-lethal interactions identify two novel genes, *SLA1* and *SLA2*, that control membrane cytoskeleton assembly in *Saccharomyces cerevisiae*. **122:**635–644.
30. **Irie, K., M. Takase, K. Lee, D. Levin, H. Araki, K. Matsumoto, and Y. Oshima.** 1993. *MKK1* and *MKK2*, which encode *Saccharomyces cerevisiae* mitogen-activated protein kinase-kinase homologs, function in the pathway mediated by protein kinase C. Mol. Cell. Biol. **13:**3076–3083.
31. **Jackson, J. B., J. M. Pollock, and R. L. Rill.** 1979. Chromatin fractionation procedure that yields nucleosomes containing near-stoichiometric amounts of high mobility group nonhistone chromosomal proteins. Biochemistry **18:**3739–3748.

32. **Kohrer, K., and H. Domdey.** 1991. Preparation of high molecular weight RNA. Methods Enzymol. **194:**398–405.
33. **Kolodrubetz, D.** Unpublished data.
34. **Kolodrubetz, D., and A. Burgum.** 1990. Duplicated *NHP6* genes of *Saccharomyces cerevisiae* encode proteins homologous to bovine high mobility group protein 1. J. Biol. Chem. **265:**3234–3239.
35. **Kolodrubetz, D., W. Haggren, and A. Burgum.** 1988. Amino-terminal sequence of a *Saccharomyces cerevisiae* nuclear protein, NHP6, shows significant identity to bovine HMG1. FEBS Lett. **238:**175–179.
36. **Kyriakis, J. M., H. App, X.-F. Zhang, P. Banerjee, D. L. Brautigan, and U. R. Rapp.** 1992. Raf-1 activates MAP kinase-kinase. Nature (London) **358:**417–421.
37. **Lange-Carter, C. A., C. M. Pleiman, A. M. Gardner, K. J. Blumer, and G. L. Johnson.** 1993. A divergence in the MAP kinase regulatory network defined by MEK kinase and Raf. Science **260:**315–319.
38. **Lee, K., K. Irie, Y. Gotoh, Y. Watanabe, H. Araki, E. Nishida, K. Matsumoto, and D. Levin.** 1993. A yeast mitogen-activated protein kinase homolog (Mpk1p) mediates signalling by protein kinase C. Mol. Cell. Biol. **13:**3067–3075.
39. **Lee, K., and D. Levin.** 1992. Dominant mutations in a gene encoding a putative protein kinase (BCK1) bypass the requirement for a *Saccharomyces cerevisiae* protein kinase C homolog. Mol. Cell. Biol. **12:**172–182.
40. **Levin, D., and B. Errede.** 1993. A multitude of MAP kinase activation pathways. J. NIH Res. **5:**49–52.
41. **Levin, D. E., and E. Bartlett-Heubusch.** 1992. Mutants in the *S. cerevisiae PKC1* gene display a cell cycle-specific osmotic stability defect. J. Cell Biol. **116:**1221–1229.
42. **Levy, B., N. C. Wong, and G. H. Dixon.** 1977. Selective association of the trout-specific H6 protein with chromatin regions susceptible to DNase I and DNase II: possible location of HMG-T in the spacer region between core nucleosomes. Proc. Natl. Acad. Sci. USA **74:**2810–2814.
43. **Lin, L.-L., M. Wartmann, A. Y. Lin, J. L. Knopf, A. Seth, and R. J. Davis.** 1993. $cPLA_2$ is phosphorylated and activated by MAP kinase. Cell **72:**269–278.
44. **Madden, K., C. Costigan, and M. Snyder.** 1992. Cell polarity and morphogenesis in *Saccharomyces cerevisiae*. Trends Cell Biol. **2:**22–29.
45. **Madden, K., and M. Snyder.** 1992. Specification of sites for polarized growth in *Saccharomyces cerevisiae* and the influence of external factors on site selection. Mol. Biol. Cell **3:**1025–1035.
46. **Mazzoni, C., P. Zarzov, A. Rambourg, and C. Mann.** 1993. The SLT2(MPK1) MAP kinase homolog is involved in polarized cell growth in *Saccharomyces cerevisiae*. J. Cell Biol. **123:**1821–1833.
47. **Neiman, A., B. J. Stevenson, H. P. Xu, G. F. Sprague, I. Herskowitz, M. Wigler, and S. Marcus.** 1993. Functional homology of protein kinases required for sexual differentiation in *Schizosaccharomyces pombe* and *Saccharomyces cerevisiae* suggests a conserved signal transduction module in eukaryotic organisms. Mol. Biol. Cell **4:**107–120.
48. **Paravicini, G., M. Cooper, L. Friedli, D. J. Smith, J.-L. Carpentier, L. S. Klig, and M. A. Payton.** 1992. The osmotic integrity of the yeast cell requires a functional *PKC1* gene product. Mol. Cell. Biol. **12:**4896–4905.
49. **Payne, D. M., A. J. Rossomando, P. Martino, A. K. Erickson, H. Jeng-Horng, J. Shabanowitz, D. F. Hunt, M. J. Weber, and T. W. Sturgill.** 1991. Identification of the regulatory phosphorylation sites in pp42/mitogen-activated protein kinase (MAP kinase). EMBO J. **10:**885–892.
50. **Pulverer, B. J., J. M. Kyriakis, J. Avruch, E. Nikolakaki, and J. R. Woodgett.** 1991. Phosphorylation of c-*jun* mediated by MAP kinases. Nature (London) **353:**670–674.
51. **Rossomando, A., J. Wu, M. Weber, and T. W. Sturgill.** 1992. The phorbol ester-dependent activator of the mitogen-activated protein kinase p42 super(mapk) is a kinase with specificity for the threonine and tyrosine regulatory sites. Proc. Natl. Acad. Sci. USA **89:**5221–5225.
52. **Rothstein, R.** 1983. One step gene disruption in yeast. Methods Enzymol. **101:**202–211.
53. **Saiki, R. K., D. H. Gelfand, S. Stoffel, S. J. Sharf, R. Higuchi, G. T. Horn, K. B. Mullis, and H. A. Elrich.** 1988. Primer-directed enzymatic amplification of DNA with a thermostable DNA polymerase. Science **239:**487–494.
54. **Saiki, R. K., S. Sharf, F. Faloona, K. B. Mullis, G. T. Horn, H. A. Erlich, and N. Arnhein.** 1985. Enzymatic amplification of β-globin genomic sequences and restriction site analysis for diagnosis of sickle cell anemia. Science **230:**1350–1354.
55. **Sambrook, J., E. F. Fritsch, and T. Maniatis.** 1989. Molecular cloning: a laboratory manual. Cold Spring Harbor Laboratory, Cold Spring Harbor, N.Y.
56. **Sanger, F., S. Nicklen, and A. R. Coulson.** 1977. DNA sequencing with chain-terminating inhibitors. Proc. Natl. Acad. Sci. USA **74:**5463–5467.
57. **Seth, A., F. A. Gonzalez, S. Gupta, D. L. Raden, and R. J. Davis.** 1992. Signal transduction within the nucleus by mitogen-activated protein kinase. J. Biol. Chem. **267:**24796–24804.
58. **Sherman, F., G. Fink, and J. Hicks.** 1986. Methods in yeast genetics. Cold Spring Harbor Laboratory, Cold Spring Harbor, N.Y.
59. **Sikorski, R., and P. Hieter.** 1989. A system of shuttle vectors and yeast host strains designed for efficient manipulation of DNA in *Saccharomyces cerevisiae*. Genetics **122:**19–27.
60. **Sloat, B., and J. Pringle.** 1978. A mutant of yeast defective in cellular morphogenesis. Science **200:**1171–1173.
61. **Snyder, M.** 1989. The SPA2 protein of yeast localizes to sites of cell growth. J. Cell Biol. **108:**1419–1429.
62. **Snyder, M., S. Gehrung, and B. D. Page.** 1991. Studies concerning the temporal and genetic control of cell polarity in *Saccharomyces cerevisiae*. J. Cell Biol. **114:**515–532.
63. **Sturgill, T. W., L. B. Ray, E. Erikson, and J. L. Maller.** 1988. Insulin-stimulated MAP-2 kinase phosphorylates and activates ribosomal protein S6 kinase II. Nature (London) **334:**715–718.
64. **Tercero, J. C., L. E. Riles, and R. B. Wickner.** 1992. Localized mutagenesis and evidence for post-transcriptional regulation of *MAK3*. J. Biol. Chem. **267:**20270–20276.
65. **Torres, L., H. Martin, M. I. Garcia-Saez, J. Arroyo, M. Molina, M. Sanchez, and C. Nombela.** 1991. A protein kinase gene complements the lytic phenotype of *Saccharomyces cerevisiae lyt2* mutants. Mol. Microbiol. **5:**2845–2854.
66. **Tremethick, D. J., and P. L. Molloy.** 1988. Effects of high mobility group proteins 1 and 2 on initiation and elongation of specific transcription by RNA polymerase II *in vitro*. Nucleic Acids Res. **16:**11107–11123.
67. **Warner, J. R.** 1991. Labelling of RNA and phosphoproteins in *Saccharomyces cerevisiae*. Methods Enzymol. **194:**423–424.
68. **Wilson, I. A., H. L. Niman, R. A. Houghten, A. R. Cherenson, M. L. Connolly, and R. A. Lerner.** 1984. The structure of an antigenic determinant in a protein. Cell **37:**767–778.
69. **Xie, K., E. J. Lambie, and M. Snyder.** 1993. Nuclear dot antigens may specify transcriptional domains in the nucleus. Mol. Cell. Biol. **13:**6170–6179.